Journal of the European Ceramic Society xxx (xxxx) xxx–xxx

Contents lists available at ScienceDirect

Journal of the European Ceramic Society

journal homepage: www.elsevier.com/locate/jeurceramsoc

Full Length Article

Predicting powder densification during sintering

S.Y. Gómez*, D. Hotza

Department of Chemical Engineering, Federal University of Santa Catarina, 88040-900, Florianópolis, SC, Brazil

ARTICLE INFO

Keywords:
Sintering
Densification
Powder
Modeling
Simulation
Master sintering curve

ABSTRACT

The milestone of sintering studies is to predict the densification resulting from the coalescence of powder particles under different thermal histories. Although sintering is a common process to produce devices with dense and/or porous materials, predicting the outcome from a given heating procedure is still a challenge. Hence, manufacturing sintered products is currently guided by previous work at very specific experimental settings, full material characterization or trial and error approaches. Here we develop and validate a simple model to overcome those issues towards efficient thermal cycles design by predicting densification during sintering. Additionally, this model may be helpful in diverse areas beyond the scope of sintering, such as in reaction systems, and for modeling other Arrhenius-like phenomena.

1. Introduction

Sintering is a key processing step for manufacturing powder metallurgy-based products used in innumerable applications, including devices for upcoming sustainable energy scenarios as fuel cells, solar cells and electrolyzer cells. In those, as in many other applications, the development of new materials and efficient processing techniques, as well as the optimization of the device architecture are fundamental issues to be addressed [1–4]. A great deal of the efforts towards further commercialization of sintered devices lies in controlling the sintering step, which involves the adjustment of the necessary temperature and time to tailor the required connectivity, porosity or densification.

The densification of a specific material during sintering depends on several variables such as temperature, time, initial density, as well as particle size and distribution [5–7]. For instance, a similar fired bodýs density may be reached in times 10^6-10^8 shorter for powder particles of 10 nm when compared to 1 μm particles, according to Herring's scaling law [8].

The available analytical methods of the sintering process can be divided into three levels: atomic, particle and continuum [9]. Modeling and simulation of sintering generally refers to different approaches not only including distortion calculations, morphology issues or stress distribution in the sintering body but also simulating microstructural evolution [10–14], mainly densification, which is the focus of the current work.

As further discussed throughout the manuscript, the current models for densification during sintering do not follow strictly the experimental data. Moreover, available sintering data, even for the same material, are just useful for the very specific experimental settings. Hence, the common practice is to determine experimentally the appropriate conditions to meet the requirements.

Herein, we develop a practical model able to predict densification of powder-based materials. To demonstrate the concept we use available sintering data of widely used materials, such as yttria tetragonal zirconia polycrystals (YTZP), alumina and nickel. Finally, further applications of the model are also proposed.

2. Brief background and model development

The sintering process arises by heating material particles below its melting point, so that bulk-surface mobility is promoted through minimization of energy surface area, which produces a volume change (Fig. 1A). The total volume V can be defined as:

$$V_{total} = V_{solids} + V_{pores} \quad (1)$$

where V_{solids} is the solids volume, and V_{pores} the pores volume. The former volume does not change during the process, and the latter diminishes driving the volume shrinkage. Dividing Eq. (1) by the volume we have:

$$1 = \theta + \rho \quad (2)$$

where θ is the porosity, and ρ, the relative density. The structure and density evolution − from the initial density (ρ_o) up to the maximum value (ρ_∞) − is commonly split into three stages and depends on the temperature (T) and time (t) applied to the process (Fig. 1B).

The transport processes involved in sintering are considered

* Corresponding author.
E-mail addresses: sergioyesidg@gmail.com, sergio.gomez@ufsc.br (S.Y. Gómez).

http://dx.doi.org/10.1016/j.jeurceramsoc.2017.10.020
Received 28 July 2017; Received in revised form 6 October 2017; Accepted 8 October 2017

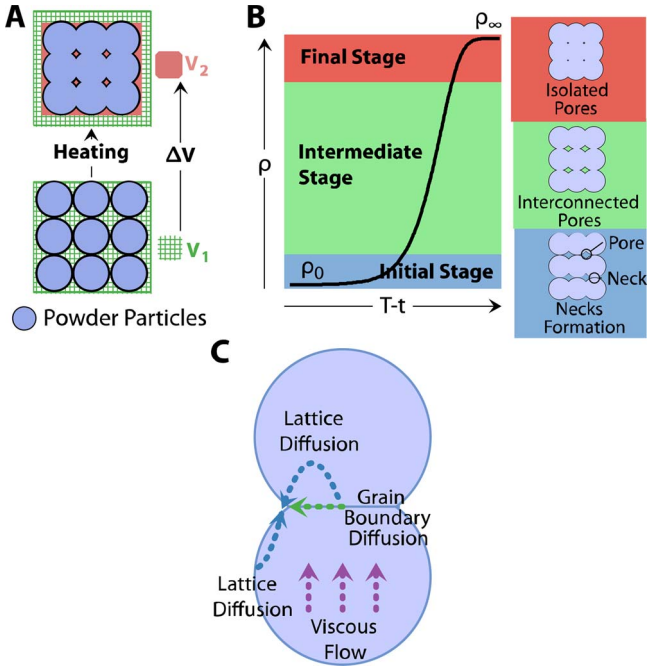

Fig. 1. Sintering stages and densification. (A) Volume shrinkage by heating the particulate compact. (B) Densification curve, density ρ_o vs. temperature (T) or time (t), where ρ_o is the green density or initial density, and ρ_∞ the final density, also showing the sintering stages. (C) Material transport paths that produce density change.

Table 1
Model constants.

Material	A	E_a (kJ mol^{-1})	n
YTZP	544.5	206.4	0.435
Alumina	2000	210	0.4
Nickel	6×10^{-5}	23	0.4

complex and still not fully understood [15]. Generally, researchers make use of theoretical approaches − mainly two-sphere models − to demonstrate the effects due to material properties and process variables. Two-sphere models diverge depending on the on-going sintering stage and the material transport path. The mechanisms known to produce densification are lattice diffusion, grain boundary diffusion, and viscous or plastic flow (Fig. 1C).

The mechanisms are described at the initial stage by Eqs. (3)–(5), based on the work of several researchers [16–20] as:

$$\frac{d\rho}{\rho} = -\left[\frac{24\gamma D_L \Omega}{RT}\right]^{1/2} \frac{t^{1/2}}{G^{3/2}} \tag{3}$$

$$\frac{d\rho}{\rho} = -\left[\frac{144\gamma D_B \Omega\delta}{RT}\right]^{1/3} \frac{t^{1/3}}{G^{4/3}} \tag{4}$$

$$\frac{d\rho}{\rho} = -\left[\frac{9\gamma}{4\eta}\right]^{1/2} \frac{t}{G} \tag{5}$$

where D_L is the lattice diffusion coefficient; D_B, the boundary diffusion coefficient; η, the viscosity; γ, the surface energy; Ω, the atomic volume; G, the particle mean diameter; δ, the boundary thickness; and R, the gases constant.

During densification more than one mechanism may be active simultaneously [21]. We propose to roughly approximate the mechanism equation to fit any case as:

$$\frac{d\rho}{\rho} = -C_1 \frac{t^n}{G} \tag{6}$$

where C_i coefficients can be rationalized as a constant that depends on the material properties, and n as a constant related to effective sintering mechanism with a value in between of 1/3 to 1. Fits from experimental data at initial sintering stage from equations similar to the proposed here, are commonly used to assess the sintering mechanism, correlating n to the respective mechanism of sintering [22,23]; viscous flow (n = 1), lattice diffusion (n = 1/2), or grain boundary diffusion (n = 1/3).

Disregarding particle-coarsening contribution to densification, Eq. (6) can be written as:

$$\frac{1}{\rho}\frac{d\rho}{\rho} = -C_1 \frac{n}{G} t^{n-1} \tag{7}$$

Combined-stage models [24,25], are valid within the three sintering stages, and described by:

$$\frac{1}{\rho}\frac{d\rho}{\rho} = -3\frac{F(\rho)}{G^m}\frac{\gamma D_o \Omega\delta}{kT}\exp\left[-\frac{E_a}{RT}\right] = -\frac{C_2}{T}\frac{F(\rho)}{G^m}\exp\left[-\frac{E_a}{RT}\right] \tag{8}$$

where D_o is the effective diffusion coefficient; k, the Boltzmann constant; E_a, the activation energy; F(ρ), the microstructural function; and m, a constant that depends on the sintering mechanism.

Eq. (8) is used to model material kinetics, and it is also the core of techniques such as two-step sintering and the master sintering curve (MSC) [26,27]. Nevertheless, the approximations or measurements for F(ρ) are currently not satisfactory. Therefore, there is a limitation for the use of the model.

The MSC is widely applied to assess the activation energy and to characterize the sintering behavior regardless time and temperature [26]. This consists on constructing a ρ vs. log(Θ) curve, using sintering data and relating it with the process based on the separation of the density and time-temperature dependencies in Eq. (8) as:

$$\Theta(t, T(t)) = \int \frac{1}{T}\exp\left[-\frac{E_{ap}}{RT}\right]dt = \Phi(\rho) \tag{9}$$

where E_{ap} is the apparent activation energy, where F(ρ) is implicit within the density function Φ. By solving Θ and relating it indirectly with the density, the MSC approach is capable to predict the achieved density for different time-temperature profiles. However, presents some limitations:

- Retrieving data is an indirect process, so it is necessary to compute new data finding the corresponding ordinate value at that point of the curve.
- Dependence on the initial and final density, i.e., if the experimenter constructs the curve with 50% initial density, the predicted values will be valid for those experiment conditions only; otherwise, an initial offset may be present.
- The activation energy do not correspond to an overall value; consequently, if having the same material but different particle size, the density predictions are over or underestimated.

Nevertheless, the MSC approach is useful and demonstrates the importance of Eq. (8), since its application has been widely used for liquid phase and solid state sintering [26,28].

For the isothermal case, we can write Eq. (8) as:

$$\frac{1}{\rho}\frac{d\rho}{dt} = -C_3 \frac{F(\rho)}{G^m} \tag{10}$$

Since Eqs. (10) and (7) are both valid at the initial sintering stage considering isothermal conditions, it is possible to infer that:

$$\frac{F(\rho)}{G^m} \approx C_4 \frac{n}{G} t^{n-1} \tag{11}$$

Replacing Eq. (11) in Eq. (8), Eq. (8) can be expressed as: